

# A Fast and Room-Temperature Operation Ammonia Sensor Based on Compound of Graphene With Polypyrrole

Xiaohui Tang<sup>1</sup>, Driss Lahem, Jean-Pierre Raskin<sup>2</sup>, *Fellow, IEEE*, Pierre Gérard, Xin Geng, Nicolas André, and Marc Debliquy

**Abstract**—We report a new hybrid sensor in which an ultrathin polypyrrole (PPy) layer is deposited on the CVD-grown graphene (G) by electropolymerization. The sensor exhibits an excellent performance in the selective sensing of ammonia (NH<sub>3</sub>) at room temperature, having a high, fast, and reversible response. It also shows rather good stability, reproducibility, and immunity to humidity. These performances are attributed to the synergistic effect between the PPy layer and G. Specifically, the NH<sub>3</sub> molecules are adsorbed on the PPy layer, electrons transfer from NH<sub>3</sub> to the PPy layer, changing the PPy layer resistance. Electrons can also be transferred to the G through the ultrathin PPy layer, in certain way changing the G resistance. These promote the sensor sensitivity. Moreover, the ultrathin PPy layer with porous nature plays an important role in the sensor response, selectivity, and immunity to humidity. Graphene is not only a support material for PPy electropolymerization but also provides an efficient pathway for electron transfer, thereby, accelerating the sensor response and recovery. Our research indicates that the combination of PPy and G is a very promising as a chemical sensor material. We implement a smart prototype with the present sensor in an electronic board for real-time monitoring the NH<sub>3</sub> concentrations. The smart prototype can be connected to a computer by a USB port for demonstrating NH<sub>3</sub> concentrations, transmitting the data and analyzing the sensor response curves. Our results are beneficial forward the commercial design and fabrication of sensors fulfilling the specifications of practical applications.

**Index Terms**—Graphene, polypyrrole, ammonia, hybrid sensor, smart prototype.

## I. INTRODUCTION

AMMONIA (NH<sub>3</sub>) is one of the most harmful pollutant gases. NH<sub>3</sub> injures the human eyes, skin, respiratory tract, liver and kidneys beyond 25 ppm concentration [1], [2].

Manuscript received July 2, 2018; revised August 28, 2018; accepted September 2, 2018. Date of publication September 10, 2018; date of current version October 23, 2018. This work was supported in part by the Multi-Sensor-Platform for Smart Building Management under Project 611887, and in part by the Walloon Region of Belgium under Captindoor Project 1217697, and Fonds Européen de Développement Régional FEDER Micro+. The associate editor coordinating the review of this paper and approving it for publication was Dr. Camilla Baratto. (*Corresponding author: Xiaohui Tang.*)

X. Tang, J.-P. Raskin, P. Gérard, and N. André are with ICTEAM, Université Catholique de Louvain, 1348 Louvain-la-Neuve, Belgium (e-mail: xiaohui.tang@uclouvain.be; jean-pierre.raskin@uclouvain.be; pierre.gerard@uclouvain.be; nicolas.andre@uclouvain.be).

D. Lahem is with the Department of Materials Science, Materia Nova ASBL, 7000 Mons, Belgium (e-mail: driss.lahem@materianova.be).

X. Geng and M. Debliquy are with the Materials Science Department, University of Mons, 7000 Mons, Belgium (e-mail: marc.debliquy@umons.ac.be; xin.geng@student.umons.ac.be).

Digital Object Identifier 10.1109/JSEN.2018.2869203

Meanwhile, it plays a decisive role in particulate matter (PM) formation. Most of NH<sub>3</sub> in our life environment is emitted directly or indirectly by chemical industries and human activities. Although plenty of NH<sub>3</sub> sensors have been studied and investigated in the literature [3], [4], it is still a great challenge to develop high performance devices. Recently, NH<sub>3</sub> sensors have found a new potential in medical applications. Specifically, NH<sub>3</sub> sensors can be used to diagnose certain diseases through detecting NH<sub>3</sub> concentration from human breath. It was reported that the patients with renal disorders or ulcers exhale NH<sub>3</sub> concentration in the range from 0.8 to 14 ppm, whereas the exhalation of the good health person is in the range of 0.15–1.8 ppm [5]. Metal oxides, catalytic metals and conducting polymers were used as sensing materials in NH<sub>3</sub> sensor fabrication. Some of them may be expensive, need high-temperature operation and high power consumption, have a short lifetime, or low selectivity. Therefore, there is an urgent requirement to develop NH<sub>3</sub> sensors which are sensitive, specific, fast, reliable, operating at room-temperature and suitable for real-life humidity condition.

Graphene (G) has attracted much attention for sensor applications. Single layer graphene with a large specific surface area of 2630 m<sup>2</sup>/g [6] provides the number of binding sites to yield high sensitivity. The graphene resistance is very sensitive to its carrier concentration. The adsorption of target molecules leads to the electron donation or withdrawal from graphene, which makes the graphene resistance significantly change. Particularly, the high carrier mobility of graphene (200 000 cm<sup>2</sup>/s.V) [7] inherently ensures low electrical noise and low power consumption. As a result, extremely small change in the graphene resistance caused by target adsorption is detectable, possessing the potential ability to detect one single molecule [8]. It is well known that pristine graphene is chemically inert and weakly binding with target molecules [9]. However, graphene is easy to be functionalized by organic compounds, such as polymers that can interact with target molecules [10]. Graphene functionalization can be either covalent or non-covalent [11]. The former disrupts graphene electronic and mechanical properties, whereas the later improves the graphene binding ability and maintains the graphene original properties simultaneously. It is important to optimize functionalization methods with non-covalent bonds, which act only as specific links.

TABLE I  
SUMMARY OF RECENT RESEARCH RESULTS FOR NH<sub>3</sub> SENSORS BASED ON PPy FILM, rGO, THEIR COMPOUNDS,  
AND RELATED MATERIALS, OPERATING AT ROOM TEMPERATURE

Sensor Type	Sensing Material	Synthesis Method	Sensitivity	Detection Limit	Response Time	Recovery Time	Reference
IDA	PPy film	Electropolymerization	55%/500ppm	8 ppm	>100 min	>120 min	[28]
IDA	PPy film	Electropolymerization	16%/40ppm	3 ppm			[29]
IDA	PPy+rGO	Chemical Reduction	2,4%/1ppb	1 ppb	1,4 s	76 s+IR	[27]
IDA	PPy nanofibers	Chemicalpolymerization		10 ppm	10 s	25 s	[30]
IDA	PPyNTs+Ag	Chemicalpolymerization	54%/40ppm	10 ppm		500 s	[31]
IDA	G-PEDOT:PSS	Chemicalpolymerization	9,6%/500ppm	5 ppm	3 min	5 min	[32]
IDA	PPy+rGO	Chemical Reduction	22%/100ppm			310 s	[33]
IDA	PANI+rGO	Chemical Reduction	37,1%/50ppm	20 ppm	18 min	2 min	[34]
IDA	PANI+G	Chemicalpolymerization	3.65/20ppm	1 ppm	50 s	27 s	[35]
IDA	PPy+s-CoPc	Electropolymerization	2%/25ppm	25 ppm	<1 min	<1min	[36]
Chemiresistor	G (CVD)		3%/500ppb		360 min	360 min	[37]
Chemiresistor	PPy+rGO	Chemical Oxidation	34,7%/500ppm	3 ppm	400 s		[26]
Chemiresistor	PPy NTs/NWs	Electropolymerization	10%/1,25ppm	1 ppm		> 40 min	[4]
Chemiresistor	PPy+rGO+TiO <sub>2</sub>	Chemicalpolymerization	102%/50ppm	1 ppm	36s	16 s	[38]
Chemiresistor	PPy+MWCN	Chemical Oxidation	3,07%/200ppm		34 s	3 min	[39]
Chemiresistor	PPy NTs/NRs	Chemical Oxidation	44%/100ppm	20 ppm	5 min	5 min	[2]
Chemiresistor	PPy/GO aerogel	Freeze dried	40%/800ppm		10 min		[40]
Chemiresistor	PANI+rGO	Chemicalpolymerization	344.2/100ppm		20 s	27 s	[41]
Chemiresistor	PPy NW	Chemicalpolymerization	0,06%/1ppm	40 ppm	15 min		[42]
FET	PPy Nribbons	Electropolymerization	2%/0.5ppm	0.5 ppm	8 min	3 min	[43]
Chemiresistor	PPy+G(CVD)	Electropolymerization	1.7%/1ppm	1 ppm	2 min	5 min	This work

G: graphene, IDE: interdigitated electrodes, FET: field-effect transistor, PANI: polyaniline, PPy: polypyrrole, rGO: reduced graphene oxide, NWs: nanowires, NRs: nanorods, NTs: nanotubes, MWCN: multi-walled carbon nanotubes, s-CoPc: n-sulfonated cobalt phthalocyanines. The rest of the abbreviations can be found in the related references.

Since the Manchester group demonstrated the detection of a single molecule (NO<sub>2</sub>) in 2007 [8], graphene-based sensors have been exploited for detecting various types of gases, for example NH<sub>3</sub>, O<sub>2</sub>, NO<sub>2</sub>, H<sub>2</sub>, CH<sub>4</sub>, SO<sub>2</sub>, H<sub>2</sub>S, and VOCs at concentrations ranging from percentage levels down to parts per billion (ppb) [12]–[16]. For the NH<sub>3</sub> sensors, the research works mainly focus on reduced graphene oxide (rGO). Although rGO can be prepared at relatively low cost and in large scale [17], the contact resistance between metal electrodes and rGO makes the sensor response complex and not well understood. The literature presents contradictory reports: Fowler *et al.* [18] claimed that the contact resistance does not influence their sensing process. Whereas Lu *et al.* [19] believed that the contact resistance contributes to the overall sensing response since the Schottky barrier variation is induced by the adsorbates.

Polypyrrole (PPy) has shown good performance for gas sensing. Apart from that, PPy is stable and biocompatible [20]. The most interesting feature of the PPy sensor is its ability to properly operate at room temperature. The first NH<sub>3</sub> sensor with PPy as sensing material goes back to 1983 by Nylander *et al.* [21]. They used a filter paper impregnated by PPy to measure NH<sub>3</sub> vapor. The compounds of rGO with PPy have been extensively exploited as electrode materials for

electrochemical supercapacitors [22], [23]. On the other hand, these materials can be used in gas sensors because of their high sensitivity, easy synthesis, and cost effectiveness [24]. Jang *et al.* [25] indicated that the improved sensitivity of the PPy/rGO sensor is mainly due to the effective electron transfer between NH<sub>3</sub> and PPy, as well as the efficient electron pathway in rGO. Tiwari *et al.* [26] further found that incorporation of rGO into PPy improves not only the sensitivity but also the response time. Although the PPy/rGO sensor reported by Hu *et al.* [27] exhibits a good sensitivity and selectivity to NH<sub>3</sub>, the sensor recovery is relatively slow (longer than 5h) in ambient condition.

According to the literature survey, we summarized in Table I the recently published NH<sub>3</sub> sensors based on G, rGO, PPy film, compounds of PPy and rGO, and related materials, operating at room temperature. For the pure PPy nanoribbon sensor, the minimum limit of detection to NH<sub>3</sub> is 0.5 ppm. Its response time and recovery time are about 8 min and 3 min, respectively. The hybrid sensors based on PPy and graphene are still rarely studied. We did not find NH<sub>3</sub> sensors made by the compound of the CVD-grown graphene and PPy. In this work, we designed a new NH<sub>3</sub> sensor, in which an ultra-thin layer of PPy is deposited on the CVD-grown graphene by electropolymerization. Hereafter, our sensor refers to the

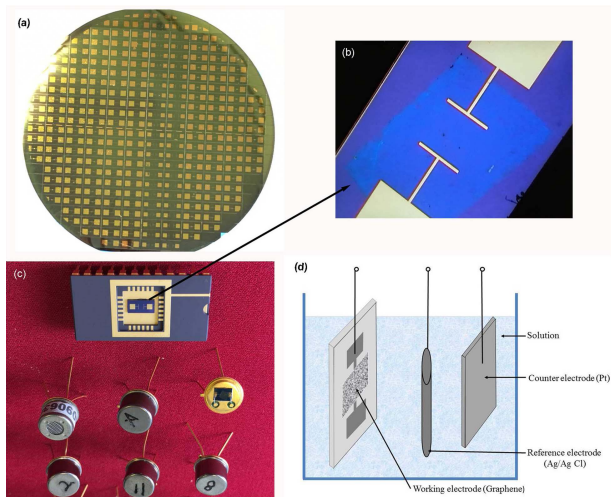


Fig. 1. (a) 3-inch Si wafer with predefined Au/Ti electrodes; (b) the CVD-grown graphene transferred on top of both electrodes; (c) PPy/G sensors bonded to TO-8 package or 24 pin dual-in-line package; and (d) a schematic illustration of electropolymerization setup.

PPy/G sensor. The sensor response, selectivity, reproducibility, and stability are examined. The influence of humidity on the sensor resistance is also tested. The key parameters of our sensors are also listed in table I for comparison purpose. We accomplished a smart prototype, which can monitor the sensor responses and the related  $\text{NH}_3$  concentrations in real-time on its liquid-crystal display. The smart prototype can also be connected to a computer by a USB port to transmit/analyze the data and show the response curves.

## II. EXPERIMENTAL

### A. Hybrid Sensor Fabrication

The fabrication of the PPy/G sensor consists of three steps: (i) the electrode deposition by a lift-off process, (ii) graphene transfer, and (iii) PPy electropolymerization. A 3-inch Si wafer is used as a starting substrate. 90-nm-thick  $\text{SiO}_2$  is thermally grown on the substrate for easily observing graphene with an optical microscope. The wafer is spin coated with positive photoresist to pattern electrodes with different sensing areas. Titanium (as an adhesion layer with the  $\text{SiO}_2$  surface) and gold layers with thicknesses of 5 and 50 nm respectively are deposited onto the photoresist. The wafer is then soaked with acetone for the lift-off process. As a result, many pairs of Au/Ti electrodes are predefined on the wafer (see Fig. 1a). The wafer is then divided into dies with an area of  $3 \times 6 \text{ mm}^2$ . Each die includes a pair of electrodes (see Fig. 1b). The graphene used for the sensor fabrication is grown on a Cu foil by CVD with methane as a precursor. The CVD-grown graphene is transferred on top of both electrodes by using poly(methyl methacrylate) (PMMA) as a mechanical support. The details of the graphene growth and transfer can be found in our previous work [44], [45]. The die with the CVD-grown graphene is glued and wire-bonded in a 24 pin dual-in-line package or TO-8 package (see Fig. 1c). Both kinds of packages can be directly contacted with our smart prototype, which will be demonstrated in the following section. It is important to point out that we use CVD-grown graphene for mass production of sensors. Moreover, the post-step graphene

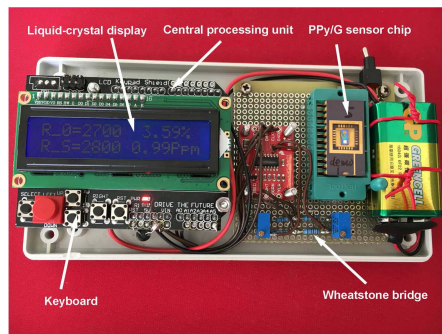


Fig. 2. A smart prototype with a PPy/G sensor for  $\text{NH}_3$  detection.

transfer is compatible with CMOS technology. These choices make it possible to design and fabricate graphene sensors with integrated circuits onto the same Si wafer in future work.

The last step in the sensor fabrication is the PPy synthesis on the CVD-grown graphene, which is carried out by electropolymerization at  $20^\circ\text{C}$ . Figure 1d illustrates the electropolymerization setup, in which the bonded die with the CVD-grown graphene is used as working electrode. The counter and reference electrodes are made of Pt and Ag/AgCl, respectively [46]. The electropolymerization bath consists of a solution of pyrrole (0.35 ml) and  $\text{NaClO}_4$  (0.6 g) in acetonitrile (50 ml). When a voltage pulse of 0.9 V is applied to the working electrode for 2 cycles, an ultrathin PPy layer of 20 nm with a porous nature is synthesized on the CVD-grown graphene. To study the effect of the PPy layer thickness on the sensor performance, a thicker PPy film with a thickness of 500 nm is also synthesized by increasing the number of voltage pulses under the same conditions. After the electropolymerization, the samples were washed with ethanol.

### B. Sensing Measurements

The relative change in resistance between the two electrodes is used to define the sensor response  $\Delta R/R_0 = (R_S - R_0)/R_0(\%)$ , where  $R_0$  and  $R_S$  are the sensor resistance before and after exposure to the target gas, respectively. The response time is defined as the time to reach 90% of the total resistance change, whereas the recovery time refers to the time required for recovering the measured resistance to 90% of its original value. Hereafter, we refer to the sensing measurements carried out at atmospheric pressure with a temperature of  $20^\circ\text{C}$  and a wet air (relative humidity of 50% RH), unless otherwise noted. Wet air and  $\text{NH}_3$  are used as carrier gas and target gas, respectively. The desired  $\text{NH}_3$  concentration is obtained by dilution of 100 ppm  $\text{NH}_3$  with wet air. For example, for 5 ppm  $\text{NH}_3$  concentration, we mix 50 ml/min of 100 ppm  $\text{NH}_3$  in air with 450 ml/min of dry air and 500 ml/min of saturated wet air (100% RH). The total gas flow is always kept at 1000 ml/min throughout a testing chamber of  $3 \text{ cm} \times 3.5 \text{ cm} \times 4 \text{ cm}$  (ca.  $42 \text{ cm}^3$  in internal volume) in all experiments.

### C. Smart Prototype Preparation

Figure 2 demonstrates our smart prototype, which includes a Wheatstone bridge, a central processing unit (CPU), a liquid-crystal display (LCD), a “keyboard”, and a PPy/G sensor. The Wheatstone bridge is biased by a 9V battery. To avoid the polarization effect on the PPy/G sensor, we ensure that

the applied voltage for the sensor is less than 0.5 V. The voltage differences across the galvanometer of the Wheatstone bridge are measured to calculate the sensor resistances  $R_0$  and  $R_S$ . Both resistances are provided to an analog-to-digital converter and then the sensor response is directly read by CPU. Using a relationship curve between  $\Delta R/R_0$  and different concentrations of  $\text{NH}_3$ , the measured gas concentrations (in ppm) can be derived and also displayed on LCD. The initial resistance of the sensor  $R_0$  is recorded in a non-volatile memory (by pressing the red bottom in the keyboard). The measurement interval is set, by default, to 1 second. This smart prototype can also be connected to a computer by a USB port for real-time monitoring, transmitting the data and analyzing the response curves of the sensors. It is worth noting that other gas sensors can be assembled with the present smart prototype.

### III. RESULTS AND DISCUSSION

#### A. Working Principle of the $\text{NH}_3$ Sensor

Schedin *et al.* reported that  $\text{NH}_3$  is an electronic donating molecule [8]. The PPy layer behaves like a *p*-type semiconductor [47]. The adsorption of  $\text{NH}_3$  on the PPy surface induces an interaction between the  $\text{NH}_3$  molecules and the PPy. The electron transfer from the  $\text{NH}_3$  molecules to the PPy layer reduces the hole concentration of the PPy layer, leading to an increase of the PPy resistance. Since the PPy electropolymerization cannot be performed directly on insulators, an intermediate layer, such as metal or graphene, must be used as a growth support. However, metallic layers are too conductive to detect small resistance changes upon exposure to  $\text{NH}_3$ . In consequence, we propose to use graphene (instead of metal) because it allows a measurable modification in resistance and tuning the PPy thickness down to nanoscale range. On the other hand, graphene behaves like a *p*-type semimetal [48]. When it is functionalized with the PPy, the electrons from the  $\text{NH}_3$  molecules can also be transferred to graphene through the PPy layer, in certain way thereby increasing the graphene resistance. We thus stack the PPy layer and graphene to combine their respective properties in a synergistic way. In summary, the ultrathin PPy layer with a porous nature plays an important role in electron exchange with  $\text{NH}_3$ , whereas graphene not only serves as a support material for PPy synthesis, but it is also an electron reservoir and a suitable pathway (i.e., not too conductive) for electron transfer.

#### B. Physical Characterization

The morphology of the CVD-grown graphene and PPy/G compound is characterized by optical microscopy and scanning electron microscopy (SEM). Figure 3a shows a top-view optical microscopy image of the CVD-grown graphene before the PPy synthesis. It can be seen that the CVD-grown graphene is composed of isolated and contiguous hexagonal flakes. Most part of graphene is single-layer. Bi- and trilayer graphene areas are found in certain regions. Figure 3b exhibits a top-view SEM image of the PPy/G compound. The PPy layer has a thickness of about 20 nm, measured by a micro system analyzer (PolyTec MSA-500). Some cavities can be observed

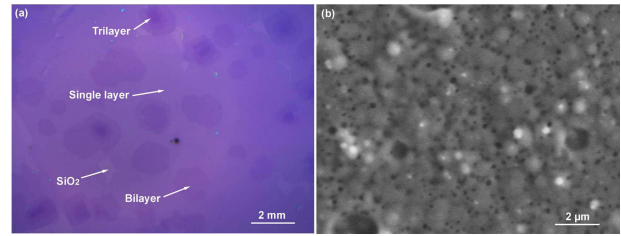


Fig. 3. (a) A top-view optical microscopy image of graphene before the PPy synthesis; and (b) a top-view SEM image of the PPy/G compound, showing a porous nature.

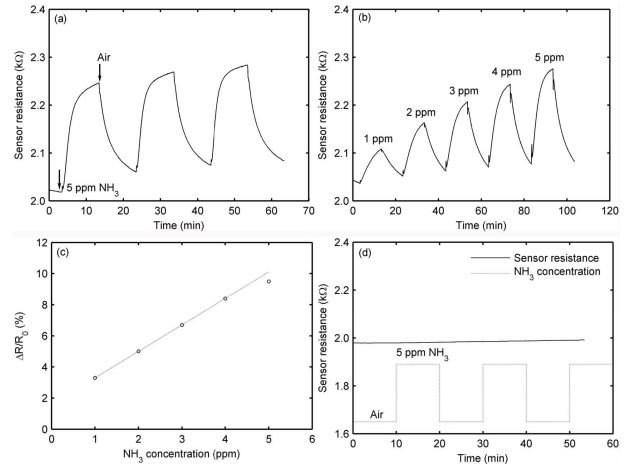


Fig. 4. Sensor behavior of a typical PPy/G sensor at relative humidity of 50% and at 20°C: (a) the sensor resistance exposed to 5 ppm  $\text{NH}_3$ ; (b) the sensor resistance exposed to  $\text{NH}_3$  concentration in a range from 1 to 5 ppm; (c) the sensor response as a function of  $\text{NH}_3$  concentration; and (d) the sensor resistance of a graphene sensor without PPy layer exposed to 5 ppm  $\text{NH}_3$ .

in the ultrathin PPy surface, which is crucial to allow the  $\text{NH}_3$  molecules to quickly come into the PPy/G compound and react with it. A detailed discussion can be found in the following sections.

#### C. Sensor Response

Figure 4a shows the resistance of the PPy/G sensor, exposed to three cycles of 5 ppm  $\text{NH}_3$ . The baseline resistance of the sensor is 2036 Ohm in wet air (50% RH at 20 °C). The  $\text{NH}_3$  exposure time is 10 min, followed by 10 min of purge with wet air. The sensor has a repeatable response of about 10%. When the PPy/G sensor is exposed to  $\text{NH}_3$ , its resistance is increased. This phenomenon is attributed to the electron transfer from the  $\text{NH}_3$  molecule to the PPy/G sensor [49]. Figure 4b and 4c present the sensor resistances and the sensor responses to different concentrations of  $\text{NH}_3$ , respectively. A linear relationship between the sensor response and  $\text{NH}_3$  concentration can be observed in the range from 1 to 4 ppm. Above concentrations of 4 ppm, the sensor response deviates from the linear curve due to the saturation of the PPy/G layer. The sensor sensitivity is evaluated to 1.7%/ppm by the slope of the linear curve. This value is comparable to those of the most sensitive  $\text{NH}_3$  sensors reported in table 1. It is emphasized that the PPy/G sensor also shows a much higher response to  $\text{NH}_3$ , compared with the graphene sensor without PPy layer (see Fig. 4d). This fact confirms that the ultrathin PPy layer plays an important role in the present sensor. Pristine graphene

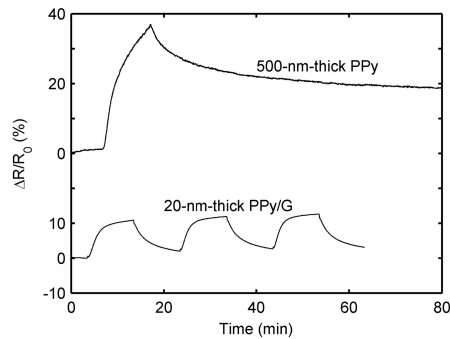


Fig. 5. Resistance responses of the PPY/G sensors with a PPY thickness of 20 nm (bottom) and 500 nm (top), exposed to 5 ppm  $\text{NH}_3$  at a relative humidity of 50% and at 20°C.

interacts very weakly with  $\text{NH}_3$  because it is chemically inert and free of dangling bonds [50]. In conclusion, the high response of our sensor is mainly attributed to the PPY layer.

#### D. Influence of PPY Thickness on Sensor Response and Recovery

We calculate the average response and recovery times of the 20-nm-thick PPY/G sensors, which are 2 and 5 min, respectively. Figure 5 displays the real-time responses to 5 ppm  $\text{NH}_3$  for the 20-nm-thick and 500-nm-thick PPY/G sensors. The response curves are shifted in the figure relatively to each other for easy comparison. Although the response of the thin PPY/G sensor is lower than that of the thick PPY sensor, the former can be fully recovered in a shorter time. The thin PPY layer provides less reactive sites for the adsorption of  $\text{NH}_3$  molecules, leading to a lower response. However, the desorption of  $\text{NH}_3$  molecules from the cavities existing in the thin PPY layer is much faster since the porous structure makes the  $\text{NH}_3$  diffusion easier and the thin PPY layer reduces diffusion pathways. The slower desorption of  $\text{NH}_3$  from the thick PPY sensor is due to the longer diffusion pathways which translate to a longer recovery time. The insufficient recovery of the thick PPY sensor would lead to unreliable sensor outputs and hysteresis effects.

It is worth noting that  $\text{NH}_3$  is mainly adsorbed on the PPY layer rather than on graphene (graphene has little affinity for  $\text{NH}_3$ ), donating electrons to the PPY layer. In turn, the PPY layer takes holes from graphene for electron recombination, depleting holes in graphene. As a result, the resistance of the PPY/G sensor is increased. During desorption,  $\text{NH}_3$  has to withdraw its electrons from the PPY layer and holes return back to graphene. So graphene serves as a reservoir allowing then a rapid electron transfer through the PPY layer. These observations may explain why the PPY/G sensor shows faster recovery time. This is one main advantage of our sensor over the thick PPY sensor. As discussed in Section I, most of the rGO-based  $\text{NH}_3$  sensors have poor reversibility, because the interaction between  $\text{NH}_3$  molecules and defects in rGO is quite strong so that thermal energy is insufficient to overcome the activation energy for the  $\text{NH}_3$  desorption [17].

Consequently, the PPY thickness has a strong influence on the PPY/G sensor response and recovery. More specifically, the thick PPY layer gives rise to high response and slow recovery. A trade-off result is that the PPY layer should be a single

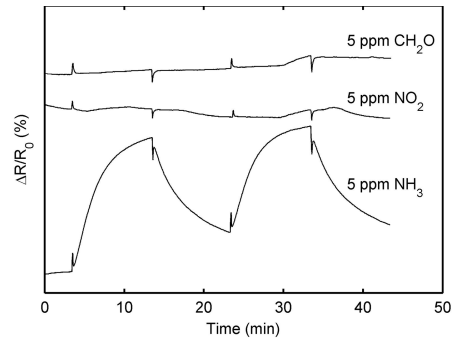


Fig. 6. Resistance responses of a typical PPY/G sensor exposed to 5 ppm  $\text{CH}_2\text{O}$ ,  $\text{NO}_2$  and  $\text{NH}_3$ , at a relative humidity of 50% and at 20°C.

layer with homogeneous and porous nature, which can expose all of its chemical bonds to the environment or the target molecules. Graphene under the thin PPY layer provides the efficient diffusion pathways for accelerating electron transfer, improving the PPY/G sensor response and recovery.

#### E. Sensor Selectivity

Schedin *et al.* indicated that graphene can interact with various molecules, including nitrogen dioxide ( $\text{NO}_2$ ) and formaldehyde ( $\text{CH}_2\text{O}$ ). The adsorption of hole donors ( $\text{NO}_2$ ) should enhance hole density in the existing p-type PPY/G compound and generate a decrease in resistance, whereas the adsorption of electron donors ( $\text{CH}_2\text{O}$ ) should cause hole depletion and hence increase in resistance [51]. We therefore investigate the PPY/G sensor selectivity towards these two gases. Figure 6 presents the PPY/G sensor response exposed to 5 ppm  $\text{CH}_2\text{O}$ ,  $\text{NO}_2$  and  $\text{NH}_3$ . For the cases of  $\text{CH}_2\text{O}$  and  $\text{NO}_2$ , no significant sensor responses are observed except for some abnormal peaks due to pressure peaks during introduction of the gases. Notice that 5 ppm of  $\text{NO}_2$  or  $\text{CH}_2\text{O}$  is much higher than the concentration in normal air conditions (less than 1 ppm). This confirms that the PPY/G sensor has an excellent selectivity to  $\text{NH}_3$  towards  $\text{CH}_2\text{O}$  and  $\text{NO}_2$ . This is associated with the fact that both  $\text{NO}_2$  and  $\text{CH}_2\text{O}$  molecules have no interaction with the PPY layer.

The presence of the ultrathin PPY layer on top of graphene hinders the interaction between interfering gases and graphene. Hernandez *et al.* [42] proved that PPY is insensitive to  $\text{NO}_2$ , since the electrostatic interaction is weak between them. Therefore,  $\text{NO}_2$  molecules can be easily desorbed from PPY. This suggests that the ultrathin PPY serves as a filtering layer, greatly improving the selectivity of the present sensor. Very small change in resistance (in Figure 6) is due to the fact that the PPY filtering layer does not perfectly cover 100% of the graphene surface area, thus small regions of graphene are exposed to the interference gases.

#### F. Humidity Effect

$\text{H}_2\text{O}$  is the most significant interfering vapor for most sensors, especially at room temperature. We tested the influence of the RH on the PPY/G sensor response. Figure 7 is the test result for the resistance variation as a function of time, exposed to 2 ppm  $\text{NH}_3$  in the range from 20 to 80% RH (the real-life RH). Table II summarizes the sensor response

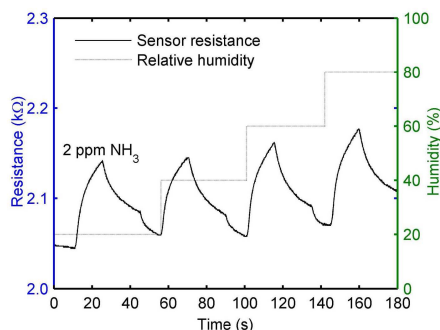


Fig. 7. Resistance behavior of a typical PPy/G sensor exposed to 2 ppm  $\text{NH}_3$  in the range from 20 to 80% RH at 20°C.

TABLE II  
SUMMARY OF THE SENSOR RESPONSE EXPOSED TO 0 AND 2 ppm  $\text{NH}_3$  AT VARIOUS RELATIVE HUMIDITY VALUES

$(R_{RH}-R_D)/R_D$ in %	RH = 20%	RH = 40%	RH = 60%	RH = 80%
$\text{NH}_3 = 0$ ppm	0.2	0.6	1.1	2.2
$\text{NH}_3 = 2$ ppm	4.2	4.5	4.9	5.2

for 0 and 2 ppm  $\text{NH}_3$  at various relative humidity values. In the table,  $R_D$  and  $R_{RH}$  are the sensor resistance under complete dry atmosphere (0% RH) and various relative humidity values, respectively. It can be seen that the response variation is about 1% in the real-life RH. Specifically, a change of 10% in RH brings a response variation of 0.17% in average. This value is 10 times smaller than the sensor sensitivity of 1.7%/ppm in wet air. We can conclude that the present sensor has a good immunity to humidity. In general, inert closed-cell  $\text{H}_2\text{O}$  can adsorb on the CVD-grown graphene through non-covalent bonds. They should influence the graphene resistance by redistributing electrons within the graphene sheet [52]. After exposure to  $\text{NH}_3$ , the adsorbed  $\text{H}_2\text{O}$  molecules interact with  $\text{NH}_3$ , making the sensing process more complicated and the sensing results unpredictable. The addition of the PPy filtering layer avoids the interaction between  $\text{H}_2\text{O}$  and graphene due to the PPy hydrophobic nature [53]. This improves the humidity immunity of the PPy/G sensor. Lin *et al.* [54] showed that the PPy resistance is not sensitive to humidity in the range from 12 to 90% RH. Sizun *et al.* [36] also reported that the PPy conductance is not sensitive to humidity in the range from 0 to 80% RH. Recently, Yin *et al.* [55] indicate that the detection capability of the PPy/rGO sensor is not severely affected by the relative humidity in the range from 0 to 80% RH. In our case, the resistance of the PPy/G hybrid material is still not sensitive to humidity in the range from 20 to 80% RH. Almost all the surface of the PPy/G sensor is uniformly covered by the PPy filtering layer. This explains why the PPy/G sensor shows only a small fluctuation to humidity variations.

#### G. Sensor Stability and Process Reproducibility

The present sensor is stable in ambient air since its resistance response almost keeps 12% for 5 ppm  $\text{NH}_3$  after one year, as shown in Fig. 8a. It can also be seen that after one year the sensor recovery seems to become slower. This may be due to the surface pollution since the sensor was left in

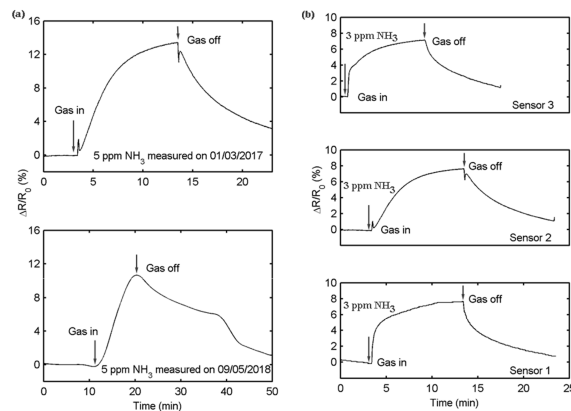


Fig. 8. (a) Resistance response of a typical PPy/G sensor exposed to 5 ppm  $\text{NH}_3$  at 20°C and 50% RH, top measured on 01/03/2017 and bottom on 09/05/2018; (b) Resistance response of three typical PPy/G sensors exposed to 3 ppm  $\text{NH}_3$  at 20°C and 50% RH, three sensors were fabricated in different batches under the same conditions.

ambient air without any protection. Although the sensor was not submitted to the same cycle, its sensitivity is similar.

To transfer the present sensor from laboratory concept to industrial application, it is necessary to investigate the process reproducibility. Therefore, we performed 3 experiments under the same conditions. Figure 8b demonstrates the resistance response of 3 typical PPy/G sensors from different batches, exposed to 3 ppm  $\text{NH}_3$  at 20°C and 50% RH. These results indicate that the present process is quite reproducible.

#### IV. CONCLUSION

In this work, we developed a new hybrid sensor, in which a 20-nm-thick polypyrrole (PPy) layer is synthesized on top of the CVD-grown graphene (G) by electropolymerization. The sensor shows a linear response for ammonia ( $\text{NH}_3$ ) in the range from 1 to 4 ppm at room temperature, with a sensitivity of 1.7%/ppm, response and recovery times of 2 and 5 min, respectively. The sensor exhibits structural stability and durability for at least one year. The sensor has a strong immunity to humidity and a good selectivity for  $\text{NH}_3$  towards interface gases ( $\text{CH}_2\text{O}$  and  $\text{NO}_2$ ). The ultrathin PPy layer with a porous nature plays an important role in the sensor sensitivity, selectivity and immunity to humidity. Graphene not only serves as a support material for PPy electropolymerization, but also accelerates the electron transport, shortening the response/recovery times. Apart from that, the ultrathin PPy layer on graphene allows the  $\text{NH}_3$  molecules to pass through the cavities to react with  $\text{sp}^2$ -bonded carbon atoms of graphene. This synergistic effect may multiply the reaction between  $\text{NH}_3$  and the PPy/G compound, thereby increasing the sensor sensitivity. Moreover, low contact resistance of graphene with Au electrode results in a high signal/noise ratio and low energy consumption. Our results indicate that the simultaneous use of PPy and graphene (the PPy/G compound) is promising as a chemical sensor material. We implement a smart prototype with the present sensor in an electronic board able to display the  $\text{NH}_3$  concentrations *in situ* and transmit the data to a computer for real-time monitoring via a USB port. This research is a step for the commercial design and mass production of room temperature  $\text{NH}_3$  sensors.

## ACKNOWLEDGMENT

The authors would like to thank the staff of UCL's Winfab and Welcome for technical support. They would also like to thank Miloud Zitout for sensors wire bonding and Nicolas Reckinger for useful discussion.

## REFERENCES

- [1] T. H. Risby and S. F. Solga, "Current status of clinical breath analysis," *Appl. Phys. B, Lasers Opt.*, vol. 85, nos. 2–3, pp. 421–426, Nov. 2006.
- [2] R. Ishpal and A. Kaur, "Spectroscopic investigations of ammonia gas sensing mechanism in polypyrrole nanotubes/nanorods," *J. Appl. Phys.*, vol. 113, no. 9, p. 094504, Mar. 2013.
- [3] B. Timmer, W. Olthuis, and A. van den Berg, "Ammonia sensors and their applications—A review," *Sens. Actuators B, Chem.*, vol. 107, no. 2, pp. 666–677, Jun. 2005.
- [4] L. Piroux, V.-A. Antohe, E. Ferain, and D. Lahem, "Self-supported three-dimensionally interconnected polypyrrole nanotubes and nanowires for highly sensitive chemiresistive gas sensing," *RSC Adv.*, vol. 6, no. 26, pp. 21808–21813, 2016.
- [5] N. Chartuprayoon, C. M. Hangarter, Y. Rheem, H. Jung, and N. V. Myung, "Wafer-scale fabrication of single polypyrrole nanoribbon-based ammonia sensor," *J. Phys. Chem. C*, vol. 114, no. 25, pp. 11103–11108, Jul. 2010.
- [6] H. S. S. R. Matte, K. S. Subrahmanyam, and C. N. R. Rao, "Synthetic aspects and selected properties of graphene," *Nanomater. Nanotechnol.*, vol. 1, no. 1, pp. 3–13, Jul. 2011.
- [7] C. Soldano, A. Mahmood, and E. Dujardin, "Production, properties and potential of graphene," *Carbon*, vol. 48, no. 8, pp. 2127–2150, Jul. 2010.
- [8] F. Schedin *et al.*, "Detection of individual gas molecules adsorbed on graphene," *Nature Mater.*, vol. 6, no. 9, pp. 652–655, Sep. 2007.
- [9] D. S. L. Abergel, V. Apalkov, J. Berashevich, K. Ziegler, and T. Chakraborty, "Properties of graphene: A theoretical perspective," *Adv. Phys.*, vol. 59, no. 4, pp. 261–482, Jul. 2010.
- [10] Y. Yang, A. M. Asiri, Z. Tang, D. Du, and Y. Lin, "Graphene based materials for biomedical applications," *Mater. Today*, vol. 16, no. 10, pp. 365–373, Oct. 2013.
- [11] V. Georgakilas *et al.*, "Functionalization of graphene: Covalent and non-covalent approaches, derivatives and applications," *Chem. Rev.*, vol. 112, no. 11, pp. 6156–6214, 2012.
- [12] C. W. Chen *et al.*, "Oxygen sensors made by monolayer graphene under room temperature," *Appl. Phys. Lett.*, vol. 99, no. 24, p. 243502, 2011.
- [13] J. Hong, S. Lee, J. Seo, S. Pyo, J. Kim, and T. Lee, "A highly sensitive hydrogen sensor with gas selectivity using a PMMA membrane-coated Pd nanoparticle/single-layer graphene hybrid," *ACS Appl. Mater. Interfaces*, vol. 7, no. 6, pp. 3554–3561, Jan. 2015.
- [14] P. A. Pandey, N. R. Wilson, and J. A. Covington, "Pd-doped reduced graphene oxide sensing films for H<sub>2</sub> detection," *Sens. Actuators B, Chem.*, vol. 183, pp. 478–487, Jul. 2013.
- [15] L. Huang *et al.*, "Multifunctional graphene sensors for magnetic and hydrogen detection," *ACS Appl. Mater. Interfaces*, vol. 7, no. 18, pp. 9581–9588, May 2015.
- [16] X. Tang, N. Mager, B. Vanhorenbeke, S. Hermans, and J.-P. Raskin, "Defect-free functionalized graphene sensor for formaldehyde detection," *Nanotechnology*, vol. 28, no. 5, p. 055501, Feb. 2017.
- [17] G. Ko, Y. Jung, K.-Y. Lee, K. Lee, and J. Kim, "Improved sorption characteristics of NH<sub>3</sub> molecules on the solution-processed graphene sheets," *J. Cryst. Growth*, vol. 326, no. 1, pp. 208–211, Jul. 2011.
- [18] J. D. Fowler, M. J. Allen, V. C. Tung, Y. Yang, R. B. Kaner, and B. H. Weiller, "Practical chemical sensors from chemically derived graphene," *ACS Nano*, vol. 3, no. 2, pp. 301–306, Feb. 2009.
- [19] G. Lu, L. E. Ocola, and J. Chen, "Reduced graphene oxide for room-temperature gas sensors," *Nanotechnology*, vol. 20, no. 44, p. 445502, 2009.
- [20] S. A. Zaidi and J. H. Shin, "Molecularly imprinted polymer electrochemical sensors based on synergistic effect of composites synthesized from graphene and other nanosystems," *Int. J. Electrochem. Sci.*, vol. 9, no. 8, pp. 4598–4616, 2014.
- [21] C. Nylander, M. Armgarth, and I. Lundström, "An ammonia detector based on a conducting polymer," in *Proc. Anal. Chem. Symp. Ser.* vol. 17, pp. 203–207, Sep. 1983.
- [22] S. Sahoo, S. Dhibar, G. Hatui, P. Bhattacharya, and C. K. Das, "Graphene/polypyrrole nanofiber nanocomposite as electrode material for electrochemical supercapacitor," *Polymer*, vol. 54, no. 3, pp. 1033–1042, Feb. 2013.
- [23] H. P. de Oliveira, S. A. Sydlik, and T. M. Swager, "Supercapacitors from free-standing polypyrrole/graphene nanocomposites," *J. Phys. Chem. C*, vol. 117, no. 20, pp. 10270–10276, May 2013.
- [24] R. L. D. Whitby, A. Korobeinyk, S. V. Mikhailovsky, T. Fukuda, and T. Maekawa, "Morphological effects of single-layer graphene oxide in the formation of covalently bonded polypyrrole composites using intermediate diisocyanate chemistry," *J. Nanoparticle Res.*, vol. 13, no. 10, pp. 4829–4837, Oct. 2011.
- [25] W.-K. Jang, J. Yun, H.-I. Kim, and Y.-S. Lee, "Improvement of ammonia sensing properties of polypyrrole by nanocomposite with graphitic materials," *Colloid Polym. Sci.*, vol. 291, no. 5, pp. 1095–1103, May 2013.
- [26] D. C. Tiwari, P. Atri, and R. Sharma, "Sensitive detection of ammonia by reduced graphene oxide/polypyrrole nanocomposites," *Synth. Met.*, vol. 203, pp. 228–234, May 2015.
- [27] N. Hu *et al.*, "Ultrafast and sensitive room temperature NH<sub>3</sub> gas sensors based on chemically reduced graphene oxide," *Nanotechnol.*, vol. 25, no. 2, p. 025502, Jan. 2014.
- [28] S. Carquigny, J. Sanchez, F. Berger, B. Lakard, and F. Lallemand, "Ammonia gas sensor based on electro synthesized polypyrrole films," *Talanta*, vol. 78, no. 1, pp. 199–206, Apr. 2009.
- [29] T. Patois, J.-B. Sanchez, F. Berger, J.-Y. Rauch, P. Fievet, and B. Lakard, "Ammonia gas sensors based on polypyrrole films: Influence of electrodeposition parameters," *Sens. Actuators B, Chem.*, vols. 171–172, pp. 431–439, Aug. 2012.
- [30] W. Wang *et al.*, "Sulfonated poly(ether ether ketone)/polypyrrole core-shell nanofibers: A novel polymeric adsorbent/conducting polymer nanostructures for ultrasensitive gas sensors," *ACS Appl. Mater. Interfaces*, vol. 4, no. 11, pp. 6080–6084, Nov. 2012.
- [31] X. Yang, L. Li, and F. Yan, "Polypyrrole/silver composite nanotubes for gas sensors," *Sens. Actuators B, Chem.*, vol. 145, no. 1, pp. 495–500, Mar. 2010.
- [32] Y. Seekaew, S. Lokavee, D. Phokharatkul, A. Wisitsoraat, T. Kercharoen, and C. Wongchoosuk, "Low-cost and flexible printed graphene-PEDOT:PSS gas sensor for ammonia detection," *Organic Electron.*, vol. 15, no. 11, pp. 2971–2981, Nov. 2014.
- [33] Y. Wang *et al.*, "Ammonia gas sensors based on chemically reduced graphene oxide sheets self-assembled on Au electrodes," *Nanosci. Res. Lett.*, vol. 9, pp. 1–12, May 2014.
- [34] X. Huang, N. Hu, L. Zhang, L. Wei, H. Wei, and Y. Zhang, "The NH<sub>3</sub> sensing properties of gas sensors based on aniline reduced graphene oxide," *Synth. Met.*, vols. 185–186, pp. 25–30, Dec. 2013.
- [35] Z. Wu *et al.*, "Enhanced sensitivity of ammonia sensor using graphene/polyaniline nanocomposite," *Sens. Actuators B, Chem.*, vol. 178, pp. 485–493, Mar. 2013.
- [36] T. Sizun, T. Patois, M. Bouvet, and B. Lakard, "Microstructured electrodeposited polypyrrole-phthalocyanine hybrid material, from morphology to ammonia sensing," *J. Mater. Chem.*, vol. 22, no. 48, p. 25246, 2012.
- [37] F. Yavari, E. Castillo, H. Gullapalli, P. M. Ajayan, and N. Koratkar, "High sensitivity detection of NO<sub>2</sub> and NH<sub>3</sub> in air using chemical vapor deposition grown graphene," *Appl. Phys. Lett.*, vol. 100, no. 20, p. 203120, May 2012.
- [38] C. Xiang *et al.*, "Ammonia sensor based on polypyrrole-graphene nanocomposite decorated with titania nanoparticles," *Ceramics Int.*, vol. 41, no. 5, pp. 6432–6438, Jun. 2015.
- [39] S. G. Bachhav and D. R. Patil, "Study of polypyrrole-coated MWCNT nanocomposites for ammonia sensing at room temperature," *J. Mater. Sci. Chem. Eng.*, vol. 03, no. 10, pp. 30–44, 2015.
- [40] L. Zhang *et al.*, "Electrosynthesis of graphene oxide/polypyrrole composite films and their applications for sensing organic vapors," *J. Mater. Chem.*, vol. 22, no. 17, p. 8438, 2012.
- [41] S. Bai *et al.*, "Ultrasensitive room temperature NH<sub>3</sub> sensor based on a graphene-polyaniline hybrid loaded on PET thin film," *Chem. Commun.*, vol. 51, no. 35, pp. 7524–7527, 2015.
- [42] S. C. Hernandez, D. Chaudhuri, W. Chen, N. V. Myung, and A. Mulchandani, "Single polypyrrole nanowire ammonia gas sensor," *Electroanalysis*, vol. 19, nos. 19–20, pp. 2125–2130, Oct. 2007.
- [43] M. Šetka, J. Drbohlavová, and J. Hubálek, "Nanostructured polypyrrole-based ammonia and volatile organic compound sensors," *Sensors*, vol. 17, no. 3, p. 562, Mar. 2017.
- [44] N. Reckinger *et al.*, "Oxidation-assisted graphene heteroepitaxy on copper foil," *Nanoscale*, vol. 8, no. 44, pp. 18751–18759, 2016.
- [45] B. Huet and J.-P. Raskin, "Pressure-controlled chemical vapor deposition of single-layer graphene with millimeter-size domains on thin copper film," *Chem. Mater.*, vol. 29, no. 8, pp. 3431–3440, Apr. 2017.

- [46] A. Decroly, A. Kruppmann, M. Debliquy, and D. Lahem, "Nanostructured TiO<sub>2</sub> layers for photovoltaic and gas sensing applications," in *Green Nanotechnology—Overview and Further Prospects*, M. L. Larramendy and S. Soloneski, Eds. Rijeka, Croatia: InTech, 2016.
- [47] M. Bazzouai, J. I. Martins, E. Machnikova, E. A. Bazzouai, and L. Martins, "Polypyrrole films electrosynthesized on stainless steel grid from saccharinate aqueous solution and its behaviour toward acetone vapor," *Eur. Polym. J.*, vol. 43, no. 4, pp. 1347–1358, Apr. 2007.
- [48] X. Tang *et al.*, "Damage evaluation in graphene underlying atomic layer deposition dielectrics," *Sci. Rep.*, vol. 5, p. 13523, Aug. 2015.
- [49] U. Latif and F. L. Dickert, "Graphene hybrid materials in gas sensing applications," *Sensors*, vol. 15, no. 12, pp. 30504–30524, Dec. 2015.
- [50] W. Fu, L. Jiang, E. P. van Geest, L. M. C. Lima, and G. F. Schneider, "Sensing at the surface of graphene field-effect transistors," *Adv. Mater.*, vol. 29, no. 6, p. 1603610, Feb. 2017.
- [51] X. Tang, J.-P. Raskin, D. Lahem, A. Kruppmann, A. Decroly, and M. Debliquy, "A formaldehyde sensor based on molecularly-imprinted polymer on a TiO<sub>2</sub> nanotube array," *Sensors*, vol. 17, no. 4, p. 675, Mar. 2017.
- [52] T. O. Wehling, M. I. Katsnelson, and A. I. Lichtenstein, "Adsorbates on graphene: Impurity states and electron scattering," *Chem. Phys. Lett.*, vol. 476, nos. 4–6, pp. 125–134, Jul. 2009.
- [53] D. Jung, M. Han, and G. S. Lee, "Humidity-sensing characteristics of multi-walled carbon nanotube sheet," *Mater. Lett.*, vol. 122, pp. 281–284, May 2014.
- [54] W.-D. Lin, H.-M. Chang, and R.-J. Wu, "Applied novel sensing material graphene/polypyrrole for humidity sensor," *Sens. Actuators B, Chem.*, vol. 181, pp. 326–331, May 2013.
- [55] Y. Yin *et al.*, "Inducement of nanoscale Cu–BTC on nanocomposite of PPy–rGO and its performance in ammonia sensing," *Mater. Res. Bull.*, vol. 99, pp. 152–160, Mar. 2018.



**Jean-Pierre Raskin** (M'97–SM'06–F'14) was born in Aye, Belgium, in 1971. He received the Industrial Engineer degree from the Institut Supérieur Industriel d'Arlon, Belgium, in 1993, and the M.S. and Ph.D. degrees in applied sciences from the Université Catholique de Louvain (UCL), Louvain-la-Neuve, Belgium, in 1994 and 1997, respectively. From 1994 to 1997, he was a Research Engineer with the Microwave Laboratory, UCL. He was involved in the modeling, characterization, and fabrication of MMIC's in Silicon-on-Insulator (SOI) technology for low-power and low-voltage applications. In 1998, he joined the EECS Department, University of Michigan, Ann Arbor, MI, USA. He has been involved in the development and characterization of micromachining fabrication techniques for microwave and millimeter-wave circuits and microelectromechanical transducers/amplifiers working in harsh environments. In 2000, he joined the Microwave Laboratory, UCL, as an Associate Professor, and has been a Full Professor since 2007. From 2009 to 2010, he was a Visiting Professor at Newcastle University, Newcastle Upon Tyne, U.K. He was the Head of the Electrical Engineering Department, UCL, from 2014 to 2017.

He has authored or co-authored over 300 scientific journal articles. His research interests are the modeling, wideband characterization and fabrication of advanced SOI MOSFETs, as well as micro and nanofabrication of MEMS/NEMS sensors and actuators, including the extraction of intrinsic material properties at nanometer scale. He is a EuMA Associate Member, the Société de l'électricité, de l'Électronique et des Technologies de L'information et de la Communication Member, and a Material Research Society Member. He was a recipient of the Médaille BLONDEL 2015, a famous French Reward that honors each year a researcher for outstanding advances in science which have demonstrated a major impact in the electrical and electronics industry. He received the SOI Consortium Award 2016 and the European SEMI Award 2017 in recognition in his vision and pioneering work for RF SOI. In 2017, he received the prestigious European Global Education Innovation Award with the NGO Louvain Cooperation.



**Xiaohui Tang** received the Ph.D. degree in applied sciences from the Université Catholique de Louvain, Belgium, in 2001. From 1983 to 1984, she was an Assistant, and worked at Kunming University of Technology, China. From 1988 to 1994, she was with the Kunming Institute of Physics, China, where she has been working on II–VI compound semiconductor materials and devices. She then was a free researcher at IMEC, Leuven, Belgium, in 1995. She is currently with the ICTEAM Institute, Université Catholique de Louvain, Belgium, as a Senior

Researcher. She has over 120 publications in international journals and conferences, five book chapters, and five patents. Her current interests are in characterization and fabrication and innovation of gas sensors and smart prototypes.



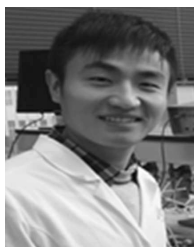
**Pierre Gérard** was working in the industry as a R&D engineer in microcontrollers programming and interfacing for 25 years. Since 2006, he has been with the Devices Integrated and Electronic Circuits Department, School of Engineering, Université Catholique de Louvain, Louvain-la-Neuve, Belgium. In 2009, he joined the Wallonia Electronics and Communications Measurements - WELCOME platform as a Systems Engineering and Integration Specialist. His main jobs are design of prototypes and demonstrators for sensors at hardware, firmware

and software level, and measurement setup software. His current interests are in wireless sensors networks and sensors interfacing.



**Driss Lahem** received the Ph.D. degree in the field of organic chemistry from the University of Mons-Hainaut, Mons, Belgium, in 1999. Since 2000, he has been with Materia Nova, Mons, a Research Center in the field of materials. He is the Scientific Leader for the research activities in the field of active coatings. He is also the co-founder of the spin-off company B-Sens ([www.b-sens.be](http://www.b-sens.be)) developing and manufacturing sensors based on optical fiber. He has authored or co-authored over 50 scientific papers and two patents. His main research areas are the

development and the validation of active materials, especially for chemical sensing and pollutants degradation.



**Xin Geng** received the B.S. degree at Yangzhou University, China, in 2013. He is currently pursuing the joint Ph.D. degree with the University of Mons, Belgium, and Yangzhou University. His research interests are in smart materials for room temperature gas sensors.



**Nicolas André** received the M.S. degrees in electrical engineering from the Louvain School of Engineering, Université Catholique de Louvain (UCL), Louvain-la-Neuve, Belgium, in 2004, and the Ph.D. degree in applied sciences in the field of micro-electromechanical systems (MEMS) co-integration from UCL in 2011. From 2011 to 2012, he was with UdeS, Sherbrooke, Canada, as a Post-Doctoral Researcher on bio-inspired methods to improve the LED efficiency. He has co-authored over 100 research papers in international journals and

holds two patents. He was a team member in several Walloon, FEDER, and EU projects as CAVIMA, STARFLO+, SHC, FEDER MINATIS, and MICRO+, and FP7 SOI-HITS. His expertise is about microfabrication and sensors (flow, humidity, pressure, light) integrated with SOI CMOS Circuits.



**Marc Debliquy** received the master's degree in chemical engineering from the Faculté Polytechnique de Mons (Faculty of Engineering) in 1994, and the Ph.D. degree in "Science de l'Ingénieur" from the Faculty of Engineering, Mons, in 1999. He joined the private company Sochinor as the Technical Manager in 2000. In 2003, he joined Materia Nova, where he was responsible for the research activities in the field of gas sensors. Since 2008, he has been with the Material Science Department, Faculty of Engineering, University of Mons, as a

Lecturer and worked as the Team Leader for the Semiconductor and Sensor Group. He was promoted as a part time Associate Professor in 2013. He teaches solid state physics and nanotechnologies. His main research interests are smart coatings for chemical detection. He has authored or co-authored 52 papers in international journals, 10 book chapters, and 60 proceedings in high level international conferences. He is also the Co-Founder of the spin-off company B-Sens ([www.b-sens.be](http://www.b-sens.be)) dealing with optical fiber sensors and semiconductor sensors. B-Sens received the Innovation Prize 2014 at the SPIE Conference in Brussels, Belgium.